CJC Chinese Journal of Chemistry 中国化学 · An International Journal

For submission: https://wiley.atyponrex.com/journal/CJOC
For published articles: https://onlinelibrary.wiley.com/journal/16147065

Concise Report

Cite this paper: *Chin. J. Chem.* **2025**, *43*, 97—103. **DOI: 10.1002/cjoc.202400796**

Photocatalytic Aldehyde Allylation for Site-Specific DNA Functionalization

Yixin Zhang,[‡,a] Ying Huang,[‡,a] Qiaoling Che,[‡,a,b] and Yiyun Chen*[,a,b,c]

[a] *State Key Laboratory of Chemical Biology, Shanghai Institute of Organic Chemistry, University of Chinese Academy of Sciences, Chinese Academy of Sciences, 345 Lingling Road, Shanghai 200032, China*
[b] *School of Physical Science and Technology, ShanghaiTech University, 100 Haike Road, Shanghai 201210, China*
[c] *School of Chemistry and Material Sciences, Hangzhou Institute for Advanced Study, University of Chinese Academy of Sciences, 1 Sub-lane Xiangshan, Hangzhou, Zhejiang 310024, China*

Keywords

DNA functionalization | Photocatalysis | Site-specific modification | Aldehyde | Nucleic acids | Allylation | DNA

Comprehensive Summary

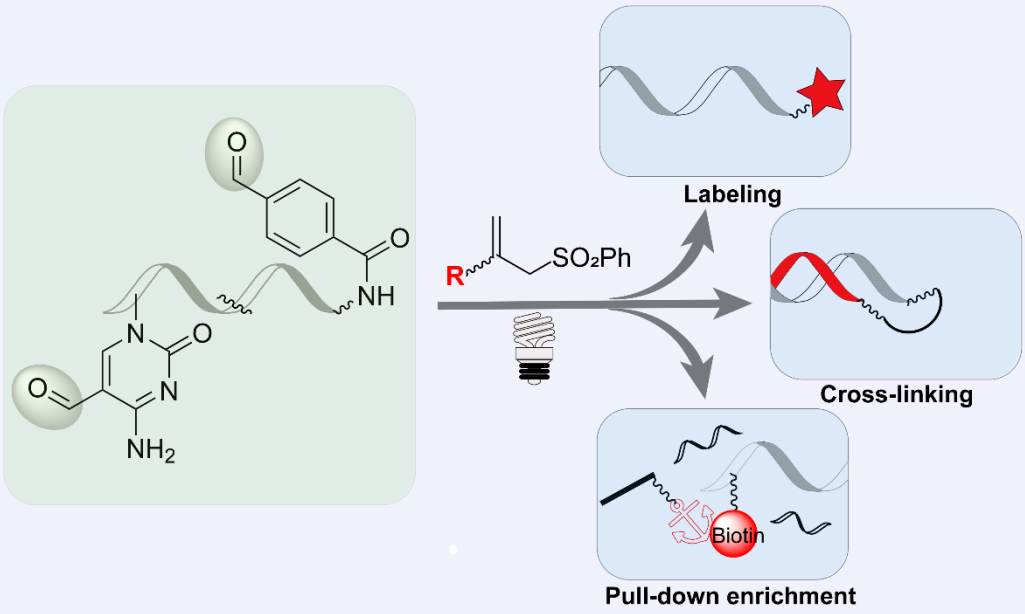

Enhancing the DNA toolbox with innovative photochemical reactions is pivotal for advancing nucleic acid-based technologies. Aldehyde groups, versatile bioorthogonal handles for imine formation under acidic conditions, are particularly valuable due to their roles in nucleic acid epigenetics. Here, we present the first photocatalytic on-DNA aldehyde allylation, enabling precise DNA functionalization under mild, neutral aqueous conditions. Our approach utilizes a photocatalytic polarity-reversal reaction between DNA-conjugated benzaldehydes and allyl sulfones. This reaction demonstrates exceptional chemoselectivity while preserving DNA integrity. By varying allyl sulfones, we achieve site-specific labeling of non-native DNA with the aldehyde group and cross-linking with DNA-bearing allyl sulfones. Furthermore, our method facilitates selective labeling and pull-down enrichment of 5-formylpyrimidine nucleotides among complex cellular DNA. This photocatalytic on-DNA aldehyde transformation expands the limited bioorthogonal photochemical toolboxes, providing novel avenues for functionalizing both non-native and native aldehyde modifications on DNA.

*E-mail: yiyunchen@sioc.ac.cn
[‡]These authors contributed equally.

© 2024 SIOC, CAS, Shanghai, & WILEY-VCH GmbH

Background and Originality Content

Precise DNA modification is a cornerstone of advancing nucleic acid-based technologies, including oligonucleotide therapeutics, drug screening, biosensing, and nanozyme catalysis.[1] Effective DNA modification reactions must operate under mild, aqueous conditions, maintain chemoselectivity, and preserve DNA sequence integrity for downstream applications.[2] Various chemical reactions have been employed to modify natural DNA, shedding light on its functions and dynamics. Additionally, non-native DNA modification has enabled the design of novel functional oligonucleotides.[3] Photochemical reactions, renowned for their mild conditions, ease of operation, and high spatiotemporal resolution, offer significant advantages for cellular applications.[2a,4] Despite advancements in synthetic photochemistry, current light-induced tools for site-specific nucleic acid modification remain limited, especially those suitable for both native and non-native DNA functionalization.[5] Therefore, exploring novel photochemical methods to expand the DNA toolbox is imperative for addressing the diverse needs of emerging nucleic acid-based technologies.

Aldehydes as functional groups are attractive for biomolecule modification due to their electrophilicity, ease of incorporation, and stability in biological systems.[6] Their natural occurrence and pivotal roles in nucleic acid epigenetics make them particularly valuable for modifying nucleic acids.[3c,7] Traditional approaches for nucleic acid labeling with aldehydes often involve amine, hydrazide, or aminoxyl derivatives (Scheme 1a).[8] However, the resulting imine formation is susceptible to hydrolysis under physiological conditions.[9] To enhance imine stability and optimize reaction kinetics, reactions are typically conducted at slightly acidic pH (4—6) or with the aid of aniline as a nucleophilic catalyst.[10] Leveraging light to drive aldehyde transformations presents an advantageous alternative to traditional acidic catalysis methods, enabling reactions under neutral conditions (Scheme 1a). Cheng and coworkers demonstrated the selective labeling of 5-formylpyrimidine RNA at neutral pH using 2-aminobenzenethiol or triphenyl phosphonium under visible or UV light, respectively.[11] The resulting products exhibited excellent fluorescence properties, facilitating the labeling and visualization of 5-formylcytidine RNA

Scheme 1 Aldehyde transformation for site-specific DNA functionalization

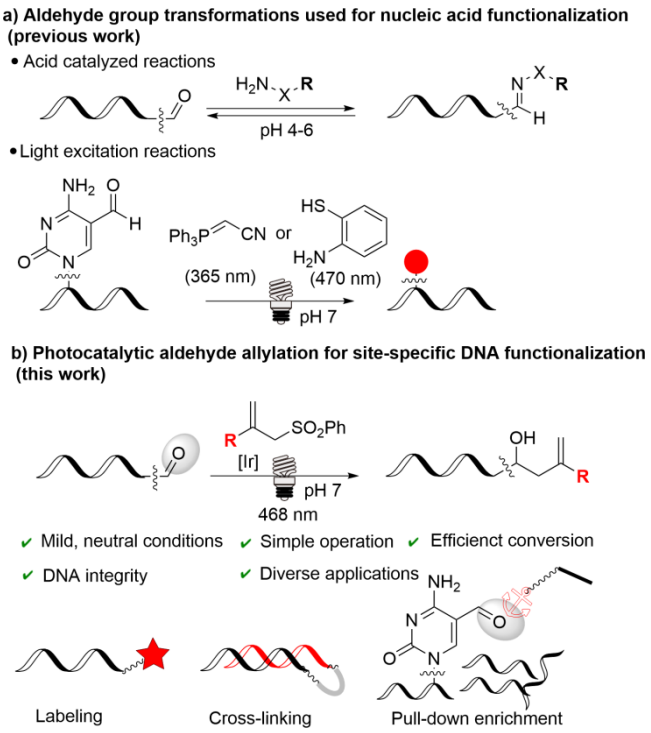

(f^{5}C). However, these approaches were limited to a narrow range of substrates, with only 2-aminobenzenethiol and triphenyl phosphonium being effective. Moreover, the direct light excitation reactions were restricted to labeling 5-formylpyrimidine in nucleic acids, hindering their broader application in DNA functionalization beyond epigenetics probing.[12] Thus, developing novel, biocompatible photocatalytic aldehyde transformation methods for DNA is essential to address the diverse needs of DNA functionalization applications.

Photocatalysis offers a promising avenue for accessing highly reactive intermediates, enabling various biocompatible chemical transformations under mild, aqueous conditions and visible light irradiation.[13] Our previous work demonstrated the photocatalytic polarity-reversed allylation of aldehydes using allyl sulfones, wherein aldehydes generated hydroxymethyl radicals through Hantzsch ester (HE) and [Ir(dtbbpy)(ppy)$_2$]PF$_6$, which subsequently added to allyl sulfones to produce homoallylic alcohols.[14] Additionally, our earlier exploration highlighted the excellent compatibility of these photocatalytic reaction conditions with nucleic acids.[15] Building upon these findings, we proposed employing the photocatalytic polarity-reversed allylation reaction for on-DNA aldehyde transformations. This approach, applicable to various substrates under mild, neutral conditions, is expected to facilitate DNA modifications. Herein, we present the first photocatalytic on-DNA aldehyde allylation via the polarity-reversal reaction, enabling site-specific functionalization of both native and non-native DNA (Scheme 1b).

Results and Discussion

Inspired by our previous work on photocatalytic on-DNA polarity-reversal allylation,[15] we initially evaluated the reactivity of DNA-conjugated benzaldehyde **DNA 1** with aryl-substituted allyl sulfone **a** (Figures S1 and S2, Table S1). While the desired allylation products were obtained in 29% yield, their yield was lower than that observed with DNA-conjugated allyl sulfone for on-DNA polarity reversal allylation. To enhance reaction efficiency, we tested benzyl ester-substituted allyl sulfone **b** and ethyl ester-substituted allyl sulfone **c** (Figure S2). Introducing alkyl ester substitution improved the reaction, with substrate **c** yielding higher. We then optimized the reaction conditions using **c** as a model substrate. We found that decreasing the photocatalyst concentration led to a significant increase to 94% yield, likely due to reduced DNA degradation at lower photocatalyst concentrations (Table 1, entries 1—2). Furthermore, the photocatalytic reactions proceeded efficiently under open-air conditions in a 50% aqueous DMF solution, demonstrating comparable yields to those obtained under a nitrogen atmosphere (entry 3). Using an aqueous MeCN solution resulted in a slightly lower 91% yield (entry 4). Similarly, reducing light irradiation to 1 h yielded up to 90% (entry 5), while high-energy blue light irradiation shortened the reaction time to 5 min with a moderate yield (entry 6). Control experiments confirmed the necessity of the photocatalyst, light, and an aldehyde-containing DNA molecule for the reaction to occur (entries 7—9).

We further evaluated the integrity of the labeled DNA after photocatalytic reaction (Scheme 2). A 108-mer long-chain DNA-conjugated phenylaldehyde (**DNA 3**, Table S2) was subjected to the photocatalytic reaction, and the resulting product was quantified using a quantitative polymerase chain reaction (qPCR). LC-MS analysis confirmed a nearly 100% retention of **DNA 4** after 3 h of irradiation. **DNA 4** was subsequently used as a template for PCR amplification, revealing minimal differences in DNA amplification efficiency compared to the standard DNA sample. These findings suggest that the DNA structural integrity is maintained under the photocatalytic reaction conditions.

With optimized reaction conditions and confirmed DNA integrity, we explored the applicability of this photocatalytic transformation for site-specific DNA functionalization. DNA-templated

© 2024 SIOC, CAS, Shanghai, & WILEY-VCH GmbH

16147065, 2025, 1, Downloaded from https://onlinelibrary.wiley.com/doi/10.1002/cjoc.202400796 by <Shibboleth>-member@sioc.ac.cn, Wiley Online Library on [02/12/2024]. See the Terms and Conditions (https://onlinelibrary.wiley.com/terms-and-conditions) on Wiley Online Library for rules of use; OA articles are governed by the applicable Creative Commons License

Table 1 Condition screening for the on-DNA photocatalytic polarity-reversed allylation

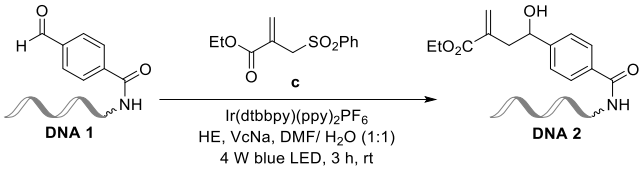

Entry	Deviation from the standard conditions[a]	Yield[b]/%
1	none	94
2	1.0 mmol/L $Ir(dtbbpy)(ppy)_2PF_6$	67
3	N_2	89
4	$MeCN/H_2O$	91
5	1 h	90
6	80 W blue light, 5 min	57
7	No light	0
8	No $Ir(dtbbpy)(ppy)_2PF_6$	9
9	instead of **DNA 1**	0

[a] Reaction conditions: **DNA 1** (1.5 nmol, 10 μmol/L), **c** (1.5 μmol, 10 mmol/L), ascorbic acid (VcNa, 7.5 μmol, 50 mmol/L), $Ir(dtbbpy)(ppy)_2PF_6$ (15 nmol, 100 μmol/L), HE (Hantzsch ester, 1.5 μmol, 10 mmol/L), H_2O/DMF = 1 : 1 (150 μL) with two blue LEDs (4 W, 468 nm) irradiation at 25 °C for 3 h. [b] Yields were determined by LC-MS analysis.

Scheme 2 DNA integrity assessment

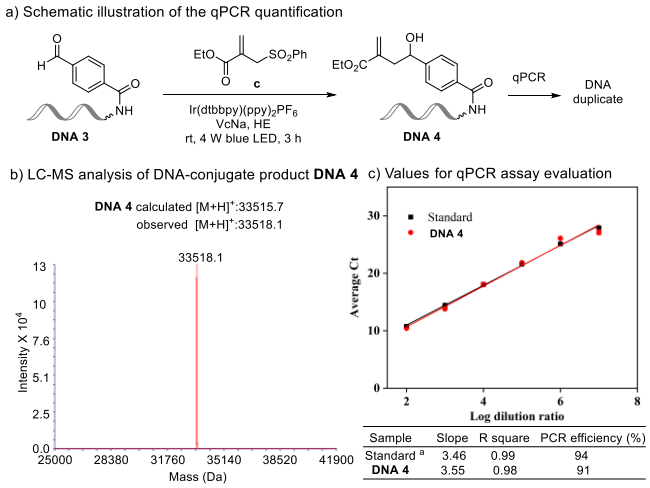

[a] A DNA conjugate without any chemical transformation served as the standard control.

synthesis, a powerful tool for the programmed creation of multiple products in a single vessel, has wide-ranging applications in nucleic acid detection, drug release, and small-molecule drug discovery.[16] By utilizing DNA hybridization to bring reactants in close proximity, DNA-templated synthesis accelerates chemical reactions under mild conditions with high chemoselectivity to facilitate DNA cross-linking. We investigated the on-DNA photocatalytic polarity-reversal reaction for DNA-templated cross-linking (Scheme 3a). Benzaldehyde and allyl sulfone scaffolds were attached to the end of the DNA C6 NH_2 template using the amidation reaction, resulting in **DNA 5** and **DNA 6**, respectively. These complementary strands hybridized to form **DNA 7**, as confirmed by native PAGE gel analysis (Scheme 3b). The increased effective molarity facilitated an efficient reaction between the aldehyde and allyl sulfone under mild blue light irradiation, producing the desired covalent cross-linking products (**DNA 8**) confirmed by urea PAGE analysis and LC-MS verification. No covalent products formed without light irradiation, and no cross-linking products were observed between mismatched template **DNA 1** and **DNA 6**. Hairpin DNA templates bearing benzaldehyde (**DNA 9**) also reacted similarly to linear DNA templates, demonstrating the versatility of the approach despite differences in the orientation of their reactive groups (Scheme 3c). Reaction products **DNA 10** were produced when the photocatalytic reaction was conducted with one equivalent of allyl sulfone (**DNA 6**) linked to a complementary **DNA 9**. These results indicated the successful application of the photocatalytic polarity-reversal reaction in DNA-templated synthesis for forming cross-links between two oligonucleotide backbones.

Scheme 3 Photocatalytic aldehyde allylation for DNA cross-linking between allyl sulfone- and aldehyde-functionalized DNA

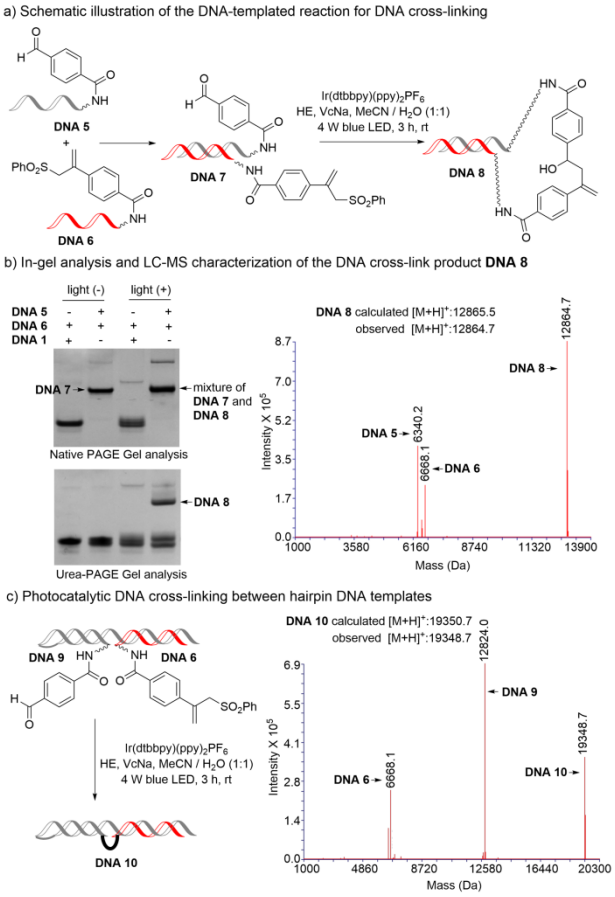

Inspired by the success of non-native DNA photo cross-linking, we hypothesized that this reaction might also label native DNA, given its reactivity with aldehyde groups. Natural nucleobase modifications, particularly aldehydes like 5-formyluracil (5fU) and 5-formylcytosine (5fC), play significant roles in epigenetics. Detecting and mapping these modifications is crucial for understanding their involvement in epigenetic regulation and disease diagnosis.[3c,17] To assess the feasibility and specificity of the allylation reactions with 5-formylpyrimidine, we subjected substrate **c** to various ribonucleosides under standard reaction conditions.[18] Gratifyingly, TBS-protected 5-formylpyrimidine nucleotides (TBS-d5fC and TBS-d5fU) were efficiently converted to their corresponding allylation products with moderate yields under visible light irradiation. In contrast, canonical ribonucleosides and other epigenetic modifications failed to react with **c** (Table S3). Additionally, *D*-ribose, a mimic of the apurinic/apyrimidinic (AP) site, showed minimal conversion, suggesting that the AP site does not interfere with 5fC detection. These results demonstrate the selective labeling and detection of 5fU and 5fC by allylation upon visi-

© 2024 SIOC, CAS, Shanghai, & WILEY-VCH GmbH

16147065, 2025, 1, Downloaded from https://onlinelibrary.wiley.com/doi/10.1002/cjoc.202400796 by <Shibboleth>-member@sioc.ac.cn, Wiley Online Library on [02/12/2024]. See the Terms and Conditions (https://onlinelibrary.wiley.com/terms-and-conditions) on Wiley Online Library for rules of use; OA articles are governed by the applicable Creative Commons License

ble light irradiation, leaving other nucleobases unreacted. Furthermore, emission intensity analysis of the photocatalytic allylation of 5-formylpyrimidine revealed a 12.3-fold fluorescence enhancement at 300 nm excitation for TBS-d5fU, while TBS-d5fC exhibited negligible spectral change (Figure S4). These distinct fluorescent emissions, potentially attributed to changes in intersystem crossing efficiency,[19] offer a promising method to differentiate between 5fC and 5fU and quantify 5fU.

Inspired by the successful chemoselective modification of the aldehyde group in nucleoside reactions, we investigated photocatalytic conjugation with a DNA strand containing 5fC modification. A 26-mer DNA strand incorporating 5fC (**DNA 11**) was synthesized via solid-phase synthesis and incubated with allyl sulfones, photocatalysts, and a reducing reagent in a 50% aqueous MeCN buffer.[20] Under blue LED light irradiation, effective conversion of 5fC within the oligonucleotide strand occurred after reaction with biotin-derived allyl sulfone **e**, as evidenced by new higher-molecular-weight bands on agarose gels (Figure S6). LC-MS analysis further confirmed a 489 Da increase in molecular weight, corresponding to the biotin modification products **DNA 12** (Scheme 4). Extending the irradiation time from 1.5 h to 3 h increased the yield, demonstrating the dose-dependency of light exposure (Table S4, entries 1—3).[21] Solvents, such as DMAC and DMF, also influenced reaction yield, with a 50% aqueous DMF buffer optimizing the reaction to 90% (Table S4, entries 4 and 5). The photocatalytic on-DNA aldehyde allylation was significantly accelerated with higher intensity irradiation; specifically, using an 80 W blue LED light for just 5 min resulted in a high yield of **DNA 12** (Table S4, entry 6). Control experiments confirmed the necessity of light and photocatalyst for the reaction, and no reaction occurred when **DNA 11** was replaced with 5fC-free DNA (Table S4, entries 7 and 8), emphasizing the inertness of coupling reactions to DNA without an aldehyde group.

Scheme 4 LC-MS characterization of converting a 26-mer DNA oligonucleotide strand containing 5fC via photocatalytic polarity-reversed allylation

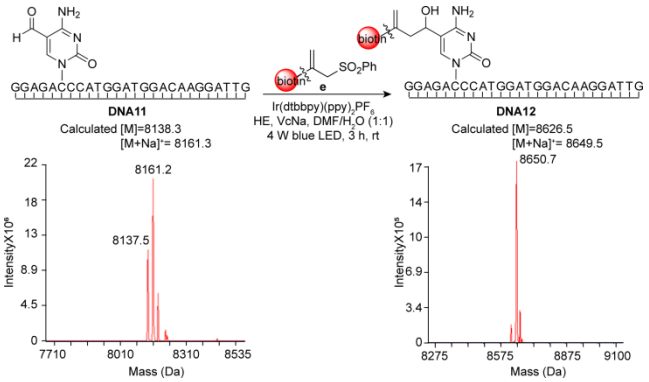

The biotin motif facilitates the isolation of modified 5fC-derived oligonucleotides through a streptavidin-based pull-down procedure, enabling their enrichment from complex mixtures.[22] To demonstrate this approach, we conducted on-DNA photocatalytic transformation with substrate **e** to enrich 5fC-containing oligonucleotides from complex mixtures. **DNA 11** was mixed with ten different non-formylated oligonucleotides at a 1 : 20 molar ratio and photo-conjugated with substrate **e** (Scheme 5a). The resulting oligonucleotide mixture was then treated with streptavidin-coated magnetic beads to immobilize all biotin-containing species, allowing for the removal of unlabeled oligonucleotides via successive washing steps. Agarose gel analysis revealed that only oligonucleotides with a molecular weight close to **DNA 11** were retained after the pull-down procedure, indicating the successful enrichment of 5fC-containing oligonucleotides (Scheme 5b, lane 4 in the left panel, lane 5 in the right panel). Control samples without the 5fC residue yielded no enriched fractions (Scheme 5b, lane 3 in the right panel). LC-MS analysis further confirmed that the enriched fractions were the corresponding biotin-modified products **DNA 12**. To simulate real biological samples, we added **DNA 11** to salmon sperm DNA, creating complex DNA mixture with a 5fC/C ratio of 0.64%. The photochemical conversion, in conjunction with the pull-down procedure, successfully captured **DNA 11** from these complex cellular DNA mixture (Figure S8). These results demonstrate that photocatalytic on-DNA allylation enables site-specific transformations of native aldehyde on DNA, offering promising avenues for studying and regulating epigenetic modifications.

Scheme 5 Pull-down enrichment of DNA containing 5fC from complex DNA mixture via photocatalytic aldehyde allylation

a) Schematic illustration of the pull-down enrichment of DNA containing 5fC

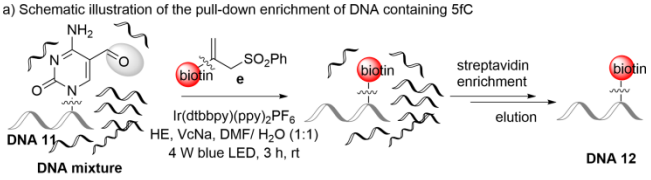

DNA **11** (10 μM)	GGAGA**5fC**CCATGGATGGACAAGGATTG-26 mer
DNA mixture (20 μM/sequence)	
TATGATAGACCCGAATTTCG-20 mer	TATGATAGACCCGAATTTCGA-21 mer
TATGATAGACCCGAATTTCGAT-22 mer	TATGATAGACCCGAATTTCGATC-23 mer
TATGATAGACCCGAATTTCGATCG-24 mer	
TATGATAGACCCGAATTTCGATCGATCGAT-34 mer	
TATGATAGACCCGAATTTCGATCGATCGATCGATC-35 mer	
TATGATAGACCCGAATTTCGATCGATCGATCGATCG-36 mer	
TATGATAGACCCGAATTTCGATCGATCGATCGATCGA-37 mer	
TATGATAGACCCGAATTTCGATCGATCGATCGATCGAT-38mer	

b) In gel analysis of pull-down enrichment samples

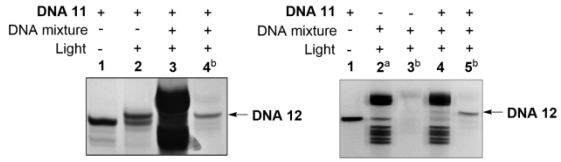

[a] **DNA 11** without aldehyde modification was added to the DNA mixture as a control. [b] Samples underwent streptavidin enrichment and elution procedures following photocatalytic reactions.

Conclusions

In conclusion, we have successfully demonstrated the first on-DNA photocatalytic aldehyde allylation. Our approach, conducted under mild, neutral aqueous conditions, efficiently transforms DNA-conjugated benzaldehydes with ethyl ester-substituted allyl sulfones, achieving yields of up to 94% while preserving DNA integrity. This novel method offers a significant advantage over traditional approaches such as Schiff base reactions,[23] Aldol-type condensation,[24] or Wittig reactions,[25] as it demonstrates comparable or superior reaction efficiency without requiring acidic conditions, high temperatures, or reliance on the native base structure. The versatility of allyl sulfones, which are compatible with various modifications including DNA and biotin, makes them ideal for DNA-templated synthesis through cross-linking non-native oligonucleotides, and selective labeling and enrichment of 5-formylpyrimidine nucleotides from complex cellular DNA. Moreover, the aldehyde group's reactivity with radical acceptors in various photocatalytic reactions suggests the potential for developing diverse DNA functionalization methods,[14,26] expanding the capabilities of nucleic acid-based technologies.

Experimental

General procedures

The supporting information presents detailed procedures for synthesizing substrate DNA and small-molecule substrates, the

 © 2024 SIOC, CAS, Shanghai, & WILEY-VCH GmbH

16147065, 2025, 1, Downloaded from https://onlinelibrary.wiley.com/doi/10.1002/cjoc.202400796 by <Shibboleth>-member@sioc.ac.cn, Wiley Online Library on [02/12/2024]. See the Terms and Conditions (https://onlinelibrary.wiley.com/terms-and-conditions) on Wiley Online Library for rules of use; OA articles are governed by the applicable Creative Commons License

photocatalytic allylation of 5-formylpyrimidine nucleotides, and the characterization of mass and NMR spectra.

Photocatalytic polarity-reversed allylation on DNA 1

DNA 1 (1.5 nmol), **c** (1.5 μmol, 15 μL, 100 mmol/L in DMF), HE (1.5 μmol, 15 μL, 100 mmol/L in DMF), $Ir(dtbbpy)(ppy)_2PF_6$ (15 nmol, 1.5 μL, 10 mmol/L in DMF), and sodium ascorbate (7.5 μmol, 15 μL, 500 mmol/L in ddH_2O) were combined in an Eppendorf tube. The mixture was adjusted to a total volume of 150 μL with DMF and water, maintaining an organic phase to aqueous phase ratio of 1 : 1. The Eppendorf tube was sealed and exposed to two blue LEDs (4 W, 468 nm, 10 cm away from the vial) at room temperature for 3 h. The mixture was then treated with 10% 5 mol/L NaCl solution and 2.5 volumes of cold ethanol (stored at −20 °C), followed by storage at −80 °C for 50 min. After centrifugation at 4 °C and 10000 r/min for 30 min, the supernatant was discarded. The precipitate was flash-frozen in liquid nitrogen and then lyophilized.

DNA integrity assessment

The qPCR test was used to evaluate the amplifiability of DNA after photocatalytic polarity-reversed allylation. The 108-mer ssDNA photocatalytic products **DNA 4** were purified by ethanol precipitation for qPCR. Samples were diluted 10-fold across 6 points, with unmodified DNA exposed to photoredox condition as a control. All samples were run in triplicate. Quantification utilized a SYBR Green Master Mix kit (Vazyme) and a QuantStudio™ 12K Flex Real-Time PCR System (Applied Biosystems, USA), with duplicate runs following manufacturer protocols in a 96-well plate. The PCR cycling parameters include 95 °C for 5 min (heat activation), followed by 40 cycles of 95 °C for 15 s (denaturation), and 60 °C for 15 s (annealing/extension). A standard curve, prepared using 108-mer control DNA quantified by Nanodrop, employed a 10-fold dilution gradient to six points, the highest concentration evaluated being 0.01 nmol/L (Table S2), with all samples similarly diluted in water and analyzed in triplicate.

DNA template synthesis

DNA 5 (2.35 nmol), **DNA 6** (2.35 nmol), HE (2.35 μmol, 23.6 μL, 100 mmol/L in DMF), $Ir(dtbbpy)(ppy)_2PF_6$ (0.235 μmol, 23.6 μL, 10 mmol/L in MeCN), and sodium ascorbate (11.75 μmol, 23.6 μL, 500 mmol/L in ddH_2O) were combined in an Eppendorf tube. The mixture was adjusted to a total volume of 235 μL with MeCN and water (organic phase to aqueous phase ratio was 1 : 1) and exposed to two blue LEDs (4 W, 468 nm, 10 cm away from the vial) at room temperature for 3 h. Subsequently, the mixture was treated with 10% 5 mol/L NaCl solution and 2.5 volumes of cold ethanol (stored at −20 °C), followed by storage at −80 °C for 50 min. After centrifugation at 4 °C and 10000 r/min for 30 min, the supernatant was discarded, and the precipitate was lyophilized after cooling in liquid nitrogen.

Procedures for labeling of 5fC-containing oligonucleotides

DNA 11 (1.5 nmol), **e** (1.5 μmol, 15 μL, 100 mmol/L in DMF), HE (1.5 μmol, 15 μL, 100 mmol/L in DMF), $Ir(dtbbpy)(ppy)_2PF_6$ (15 nmol, 1.5 μL, 10 mmol/L in DMF), and sodium ascorbate (7.5 μmol, 15 μL, 500 mmol/L in H_2O) were added to the Eppendorf tube. The mixture was supplemented with DMF and water in a total volume of 150 μL, where the ratio of organic phase to aqueous phase was 1 : 1. The Eppendorf tube was sealed and exposed to two blue LEDs (4 W, 468 nm, 10 cm away from the vial) at room temperature for 3 h. The mixture was then treated with 10% 5 mol/L NaCl solution and 2.5 volumes of cold ethanol (stored at −20 °C) and stored at −80 °C for 50 min. After centrifugation at 4 °C and 10000 r/min for 30 min, the supernatant was discarded. The precipitate was cooled in liquid nitrogen and then lyophilized.

Enrichment of 5fC-containing oligonucleotides in complex DNA

DNA 11 (1 nmol, 10 μL, 100 μmol/L in ddH_2O), DNA mixture (20 nmol, 20 μL, 0.1 mmol/L in ddH_2O), **e** (1.0 μmol, 10 μL, 100 mmol/L in DMF), HE (1 μmol, 10 μL, 100 mmol/L in DMF), $Ir(dtbbpy)(ppy)_2PF_6$ (10 nmol, 1 μL, 10 mmol/L in DMF), and sodium ascorbate (5 μmol, 10 μL, 500 mmol/L in H_2O) were combined in an Eppendorf tube. The mixture was adjusted to a total volume of 100 μL with DMF and water (organic phase to aqueous phase ratio was 1 : 1) and exposed to two blue LEDs (4 W, 468 nm, 10 cm away from the vial) at room temperature for 3 h. Subsequently, the mixture was treated with 10% 5 mol/L NaCl solution and 2.5 volumes of cold ethanol (stored at −20 °C), followed by storage at −80 °C for 50 min. After centrifugation at 4 °C and 10000 r/min for 30 min, the supernatant was discarded, and the precipitate was lyophilized after cooling in liquid nitrogen. The lyophilized precipitate was redissolved in ddH_2O, dialyzed for 24 h, and ultrafiltered 4 times. Streptavidin beads (50 μL, Dynabeads MyOne Streptavidin C1, Invitrogen) were thoroughly resuspended in a clean tube and placed on a magnet to remove the supernatant. The beads were washed four times with 200 μL 1× B&W buffer (5 mmol/L pH 7.5 Tris–HCl, 0.5 mmol/L EDTA, 1 mol/L NaCl, 0.01% Tween-20), followed by resuspension in 100 μL 2× B&W buffer (10 mmol/L pH 7.5 Tris–HCl, 1 mmol/L EDTA, 2 mol/L NaCl, 0.02% Tween-20). DNA treated from the previous step (100 μL in Milli-Q water) was combined with the bead and incubated for 15 min at room temperature with gentle rotation. After incubation, the DNA-coated beads were separated using a magnet, and the supernatant was discarded. The beads were washed five times with 200 μL 1× B&W buffer each time. To release the enriched DNA fragments, 50 μL of freshly prepared Milli-Q water was added to the coated beads, followed by incubation at −70 °C for 10 min. The supernatant was aspirated and analyzed by polyacrylamide gel electrophoresis.

Supporting Information

The supporting information for this article is available on the WWW under https://doi.org/10.1002/cjoc.202400796.

Acknowledgement

Financial support was provided by the National Natural Science Foundation of China (22337005, 22277133, 91753126), Youth Innovation Promotion Association CAS (2023266), CAS Interdisciplinary Innovation Team (JCTD-2020-16), Program of Shanghai Academic/Technology Research Leader (21XD1424700), and International Partnership Program of the Chinese Academy of Science (033GJHZ2023006FN).

References

[1] (a) Madsen, M.; Gothelf, K. V. Chemistries for DNA Nanotechnology. *Chem. Rev.* **2019**, *119*, 6384–6458; (b) Fitzgerald, P. R.; Paegel, B. M. DNA-Encoded Chemistry: Drug Discovery from a Few Good Reactions. *Chem. Rev.* **2021**, *121*, 7155–7177; (c) Li, L.; Xu, S.; Yan, H.; Li, X.; Yazd, H. S.; Li, X.; Huang, T.; Cui, C.; Jiang, J.; Tan, W. Nucleic Acid Aptamers for Molecular Diagnostics and Therapeutics: Advances and Perspectives. *Angew. Chem. Int. Ed.* **2021**, *60*, 2221–2231; (d) Loehr, M. O.; Luedtke, N. W. A Kinetic and Fluorogenic Enhancement Strategy for Labeling of Nucleic Acids. *Angew. Chem. Int. Ed.* **2022**, *61*, e202112931; (e) Larcher, L. M.; Pitout, I. L.; Keegan, N. P.; Veedu, R. N.; Fletcher, S. DNAzymes: Expanding the Potential of Nucleic Acid Therapeutics. *Nucleic Acid Ther.* **2023**, *33*, 178–192.

[2] (a) Matsuo, B.; Granados, A.; Levitre, G.; Molander, G. A. Photochemical Methods Applied to DNA Encoded Library (DEL) Synthesis. *Acc. Chem. Res.* **2023**, *56*, 385–401; (b) El-Sagheer, A. H.; Brown, T. Click chemistry with DNA. *Chem. Soc. Rev.* **2010**, *39*, 1388–1405; (c) Chen, Y.; Kamlet, A. S.; Steinman, J. B.; Liu, D. R. A biomolecule-compatible visible-light-induced azide reduction from a DNA-encoded

 © 2024 SIOC, CAS, Shanghai, & WILEY-VCH GmbH

16147065, 2025, 1, Downloaded from https://onlinelibrary.wiley.com/doi/10.1002/cjoc.202400796 by <Shibboleth>-member@sioc.ac.cn, Wiley Online Library on [02/12/2024]. See the Terms and Conditions (https://onlinelibrary.wiley.com/terms-and-conditions) on Wiley Online Library for rules of use; OA articles are governed by the applicable Creative Commons License

reaction-discovery system. *Nat. Chem.* **2011**, *3*, 146–153; (d) Huang, Y.; Savych, O.; Moroz, Y.; Chen, Y.; Goodnow, R. A., Jr. DNA-Encoded Library Chemistry: Amplification of Chemical Reaction Diversity for the Exploration of Chemical Space. *Aldrichim. Acta* **2019**, *52*, 75–87.

[3] (a) Mo, J.; Weng, X.; Zhou, X. Detection, Clinical Application, and Manipulation of RNA Modifications. *Acc. Chem. Res.* **2023**, *56*, 2788–2800; (b) McKenzie, L. K.; El-Khoury, R.; Thorpe, J. D.; Damha, M. J.; Hollenstein, M. Recent progress in non-native nucleic acid modifications. *Chem. Soc. Rev.* **2021**, *50*, 5126–5164; (c) Berney, M.; McGouran, J. F. Methods for detection of cytosine and thymine modifications in DNA. *Nat. Rev. Chem.* **2018**, *2*, 332–348; (d) Hofer, A.; Liu, Z. J.; Balasubramanian, S. Detection, Structure and Function of Modified DNA Bases. *J. Am. Chem. Soc.* **2019**, *141*, 6420–6429.

[4] (a) Fairbanks, B. D.; Macdougall, L. J.; Mavila, S.; Sinha, J.; Kirkpatrick, B. E.; Anseth, K. S.; Bowman, C. N. Photoclick Chemistry: A Bright Idea. *Chem. Rev.* **2021**, *121*, 6915–6990; (b) Reisacher, U.; Antusch, L.; Hofsass, R.; Schwechheimer, C.; Lehmann, B.; Wagenknecht, H. A. Light-induced functions in DNA. *Curr. Opin. Chem. Biol.* **2017**, *40*, 119–126; (c) Tavakoli, A.; Min, J. H. Photochemical modifications for DNA/RNA oligonucleotides. *RSC Adv.* **2022**, *12*, 6484–6507.

[5] Lechner, V. M.; Nappi, M.; Deneny, P. J.; Folliet, S.; Chu, J. C. K.; Gaunt, M. J. Visible-Light-Mediated Modification and Manipulation of Biomacromolecules. *Chem. Rev.* **2022**, *122*, 1752–1829.

[6] (a) Sletten, E. M.; Bertozzi, C. R. Bioorthogonal Chemistry: Fishing for Selectivity in a Sea of Functionality. *Angew. Chem. Int. Ed.* **2009**, *48*, 6974–6998; (b) Prescher, J. A.; Bertozzi, C. R. Chemistry in living systems. *Nat. Chem. Biol.* **2005**, *1*, 13–21.

[7] (a) Greenberg, M. V. C.; Bourc'his, D. The diverse roles of DNA methylation in mammalian development and disease. *Nat. Rev. Mol. Cell Biol.* **2019**, *20*, 590–607; (b) Xie, L. J.; Lin, C. L.; Liu, L.; Cheng, L. A chemical labeling of N^6-formyl adenosine (f^6A) RNA. *Chin. Chem. Lett.* **2022**, *33*, 1563–1566.

[8] (a) Hu, J.; Xing, X.; Xu, X.; Wu, F.; Guo, P.; Yan, S.; Xu, Z.; Xu, J.; Weng, X.; Zhou, X. Selective Chemical Labelling of 5-Formylcytosine in DNA by Fluorescent Dyes. *Chem. Eur. J.* **2013**, *19*, 5836–5840; (b) Wang, S. R.; Song, Y. Y.; Wei, L.; Liu, C. X.; Fu, B. S.; Wang, J. Q.; Yang, X. R.; Liu, Y. N.; Liu, S. M.; Tian, T.; Zhou, X. Cucurbit[7]uril-Driven Host-Guest Chemistry for Reversible Intervention of 5-Formylcytosine-Targeted Biochemical Reactions. *J. Am. Chem. Soc.* **2017**, *139*, 16903–16912.

[9] Kalia, J.; Raines, R. T. Hydrolytic stability of hydrazones and oximes. *Angew. Chem. Int. Ed.* **2008**, *47*, 7523–7526.

[10] (a) Kolmel, D. K.; Kool, E. T. Oximes and Hydrazones in Bioconjugation: Mechanism and Catalysis. *Chem. Rev.* **2017**, *117*, 10358–10376; (b) Lang, K.; Chin, J. W. Cellular Incorporation of Unnatural Amino Acids and Bioorthogonal Labeling of Proteins. *Chem. Rev.* **2014**, *114*, 4764–4806; (c) Dirksen, A.; Hackeng, T. M.; Dawson, P. E. Nucleophilic Catalysis of Oxime Ligation. *Angew. Chem. Int. Ed.* **2006**, *45*, 7581–7584.

[11] (a) Wang, R. L.; Jin, X. Y.; Kong, D. L.; Chen, Z. G.; Liu, J.; Liu, L.; Cheng, L. Visible-Light Facilitated Fluorescence "Switch-On" Labelling of 5-Formylpyrimidine RNA. *Adv. Synth. Catal.* **2019**, *361*, 5406–5411; (b) Jin, X. Y.; Huang, Z. R.; Xie, L. J.; Liu, L.; Han, D. L.; Cheng, L. Photo-Facilitated Detection and Sequencing of 5-Formylcytidine RNA. *Angew. Chem. Int. Ed.* **2022**, *61*, e202210652.

[12] (a) Zhang, J.; Liu, J.; Zhang, G.; He, X.; Xiong, F.; Fan, X.; Li, Y.; Li, Y. Synthesis of Diacylhydrazine Derivatives Based on Tetrazole-Focused DNA-Encoded Library. *Org. Lett.* **2024**, *26*, 1094–1099; (b) Zhang, J.; Liu, J.; Li, X.; Ju, Y.; Li, Y.; Zhang, G.; Li, Y. Unexpected Cyclization Product Discovery from the Photoinduced Bioconjugation Chemistry between Tetrazole and Amine. *J. Am. Chem. Soc.* **2024**, *146*, 2122–2131.

[13] (a) Mascarenas, J. L.; Mato, M.; Fernandez-Gonzalez, X.; D'Avino, C.; Tomas-Gamasa, M. Bioorthogonal Synthetic Chemistry Enabled by Visible-Light Photocatalysis. *Angew. Chem. Int. Ed.* **2024**, DOI: 10.1002/anie.202413506; (b) Hu, C.; Chen, Y. Biomolecule-compatible chemical bond-formation and bond-cleavage reactions induced by visible light. *Tetrahedron Lett.* **2015**, *56*, 884–888.

[14] Qi, L.; Chen, Y. Polarity-Reversed Allylations of Aldehydes, Ketones, and Imines Enabled by Hantzsch Ester in Photoredox Catalysis. *Angew. Chem. Int. Ed.* **2016**, *55*, 13312–13315.

[15] (a) Huang, Y.; Zhang, Y.; Hu, C.; Chen, Y. Site-specific DNA post-synthetic modification via fast photocatalytic allylation. *Org. Chem. Front.* **2024**, *11*, 4408–4415; (b) Hu, C. C.; Chen, Y. Y. Chemoselective and fast decarboxylative allylation by photoredox catalysis under mild conditions. *Org. Chem. Front.* **2015**, *2*, 1352–1355.

[16] (a) Gartner, Z. J.; Tse, B. N.; Grubina, R.; Doyon, J. B.; Snyder, T. M.; Liu, D. R. DNA-templated organic synthesis and selection of a library of macrocycles. *Science* **2004**, *305*, 1601–1605; (b) Usanov, D. L.; Chan, A. I.; Maianti, J. P.; Liu, D. R. Second-generation DNA-templated macrocycle libraries for the discovery of bioactive small molecules. *Nat. Chem.* **2018**, *10*, 704–714; (c) Ma, Z. C.; Taylor, J. S. Nucleic acid-triggered catalytic drug release. *Proc. Natl. Acad. Sci. U. S. A.* **2000**, *97*, 11159–11163.

[17] Wang, Y.; Zhang, X.; Zou, G.; Peng, S.; Liu, C.; Zhou, X. Detection and Application of 5-Formylcytosine and 5-Formyluracil in DNA. *Acc. Chem. Res.* **2019**, *52*, 1016–1024.

[18] We evaluated the reactivity of aryl- **a**, ethyl ester- **c**, and carboxyl- **d** substituted allyl sulfone with TBS-d5fC and TBS-d5fU nucleosides. Substrate **c** gave the highest yield with both TBS-d5fC and TBS-d5fU (Figure S3). Attempts to improve selectivity for 5fC and 5fU using different allyl sulfone substrates were unsuccessful.

[19] Fang, M.; Yang, J.; Li, Z. Light emission of organic luminogens: Generation, mechanism and application. *Prog. Mater. Sci.* **2022**, *125*, 100914.

[20] Similarly, the 5fC-derived oligonucleotides reacted most efficiently with substrate **c** among the substituted allyl sulfone substrates, achieving a 93% yield under optimized conditions (Figure S5).

[21] Very little DNA damage was observed under two 4 W blue LEDs at 468 nm for 3 h (Figure S7).

[22] Xia, B.; Han, D.; Lu, X.; Sun, Z.; Zhou, A.; Yin, Q.; Zeng, H.; Liu, M.; Jiang, X.; Xie, W.; He, C.; Yi, C. Bisulfite-free, base-resolution analysis of 5-formylcytosine at the genome scale. *Nat. Methods* **2015**, *12*, 1047–1050.

[23] (a) Wang, Y.; Liu, C.; Yang, W.; Zou, G.; Zhang, X.; Wu, F.; Yu, S.; Luo, X.; Zhou, X. Naphthalimide derivatives as multifunctional molecules for detecting 5-formylpyrimidine by both PAGE analysis and dot-blot assays. *Chem. Commun.* **2018**, *54*, 1497–1500; (b) Guo, P.; Yan, S. Y.; Hu, J. L.; Xing, X. W.; Wang, C. C.; Xu, X. W.; Qiu, X. Y.; Ma, W.; Lu, C. J.; Weng, X. C.; Zhou, X. Selective Detection of 5-Formyl-2′-deoxycytidine in DNA Using a Fluorogenic Hydroxylamine Reagent. *Org. Lett.* **2013**, *15*, 3266–3269.

[24] Samanta, B.; Seikowski, J.; Hobartner, C. Fluorogenic Labeling of 5-Formylpyrimidine Nucleotides in DNA and RNA. *Angew. Chem. Int. Ed.* **2016**, *55*, 1912–1916.

[25] Zhou, Q.; Li, K.; Liu, Y. H.; Li, L. L.; Yu, K. K.; Zhang, H.; Yu, X. Q. Fluorescent Wittig reagent as a novel ratiometric probe for the quantification of 5-formyluracil and its application in cell imaging. *Chem. Commun.* **2018**, *54*, 13722–13725.

[26] (a) Chen, Y.; Liu, D.; Zhang, J. Investigations on the 1,2-Hydrogen Atom Transfer Reactivity of Alkoxyl Radicals under Visible-Light-Induced Reaction Conditions. *Synlett* **2020**, *32*, 356–361; (b) Yan, Y.; Li, G.; Ma, J.; Wang, C.; Xiao, J.; Xue, D. Photoinduced generation of ketyl radicals and application in C–C coupling without external photocatalyst. *Green Chem.* **2023**, *25*, 4129–4136.

Manuscript received: July 23, 2024
Manuscript revised: September 10, 2024
Manuscript accepted: September 10, 2024
Version of record online: October 2, 2024

 © 2024 SIOC, CAS, Shanghai, & WILEY-VCH GmbH

16147065, 2025, 1, Downloaded from https://onlinelibrary.wiley.com/doi/10.1002/cjoc.202400796 by <Shibboleth>-member@sioc.ac.cn, Wiley Online Library on [02/12/2024]. See the Terms and Conditions (https://onlinelibrary.wiley.com/terms-and-conditions) on Wiley Online Library for rules of use; OA articles are governed by the applicable Creative Commons License

16147065, 2025, 1, Downloaded from https://onlinelibrary.wiley.com/doi/10.1002/cjoc.202400796 by <Shibboleth>-member@sioc.ac.cn, Wiley Online Library on [02/12/2024]. See the Terms and Conditions (https://onlinelibrary.wiley.com/terms-and-conditions) on Wiley Online Library for rules of use; OA articles are governed by the applicable Creative Commons License

The Authors



Left to Right: Yixin Zhang, Ying Huang, Qiaoling Che, and Yiyun Chen

© 2024 SIOC, CAS, Shanghai, & WILEY-VCH GmbH